NASA MEMO 1-26-59L

NASA

MEMORANDUM

FLIGHT INVESTIGATION OF THE SURFACE PRESSURE DISTRIBUTION AND FLOW FIELD AROUND AN ELLIPTICAL SPINNER

By Lovic P. Thomas III

Langley Research Center
Langley Field, Va.

NATIONAL AERONAUTICS AND SPACE ADMINISTRATION
WASHINGTON
February 1959

NATIONAL AERONAUTICS AND SPACE ADMINISTRATION

MEMORANDUM 1-26-59L

FLIGHT INVESTIGATION OF THE SURFACE PRESSURE DISTRIBUTION AND FLOW FIELD AROUND AN ELLIPTICAL SPINNER

By Lovic P. Thomas III

SUMMARY

A flight investigation has been made of the surface pressure distribution and the flow field around a dummy, nonrotating, elliptical spinner over a Mach number range from 0.65 to 0.95, which corresponds to a Reynolds number range from about 1.6×10^6 per foot to about 3.9×10^6 per foot.

The results showed that free-stream conditions were approximated from about 15 to 90 percent of the spinner length, but the local Mach number in the propeller plane varied from about 5 percent less than free stream at a Mach number of 0.65 to about 10 percent less than free stream at a Mach number of 0.95.

INTRODUCTION

Spinners have considerable influence on the propeller flow field, and a knowledge of this influence is necessary in order to analyze data obtained from propeller tests. Reference 1 shows that a conical spinner affords favorable interference to propellers because the flow is slowed in the propeller plane. Blade sections of a propeller used with the conical spinner would be operating at lower Mach numbers than a corresponding propeller outside the spinner's influence; hence, higher maximum lift-drag ratios would be available. The spinners with spherical center sections (ref. 1) caused the flow velocity to be higher than free stream in the propeller plane and, thereby, gave unfavorable interference to the propeller.

As part of an extensive propeller research program, a dummy, nonrotating, elliptical spinner was tested in flight on a propeller research airplane to determine the surface pressure distribution and the flow field around the spinner. The Mach number range of the investigation was from 0.65 to 0.95, which corresponds to a Reynolds number range from about

1.6×10^6 per foot to 3.9×10^6 per foot. The choice of an elliptical shape for the spinner was made in an attempt to minimize the interference of the spinner on the propeller. In addition, it was believed that information concerning the flow field around this elliptical shape could also be applied to other elliptical bodies such as radomes.

SYMBOLS

l length of spinner, in.

M Mach number

p static pressure, lb/sq ft

p_t total pressure, lb/sq ft

q_c impact pressure, $p_t - p_\infty$, lb/sq ft

r radius from spinner center line, in.

r_b spinner radius at blade center line, in.

x distance from nose along spinner center line, in.

y distance from spinner surface at blade center-line station, in.

$\Delta p = p_l - p_\infty$

$\frac{\Delta p}{q_c}$ static-pressure coefficient, $\frac{p_l - p_\infty}{q_c}$

Subscripts:

∞ free stream

l local

APPARATUS AND PROCEDURE

Pressure orifices were located along the length of the test spinner on both the top and bottom surfaces and static-pressure survey rakes, one on the top and one on the bottom, were installed in order that pressures could be recorded near the blade center line of a propeller to be installed with the real counterpart of this spinner. The surface and rake orifice locations are given in figure 1. A view of the installation is shown in figure 2.

Standard NACA mechanical optical differential-pressure manometers were used to measure the pressures which were accurate within ±1 percent. The airspeed and altitude of the propeller research airplane were measured by a calibrated wing-tip boom. The airplane Mach numbers obtained from this installation are accurate within ±0.005 for the range of this investigation.

In order to obtain the local Mach numbers in the plane of the propeller, it was assumed that there were no shock formations off the spinner and that the total pressure was constant. Values of local Mach number were found as functions of $q_{c,l}/p_l$, values for which, in turn, were obtained from the difference between the static pressure recorded by the rakes and that recorded by the wing-tip boom. Interference due to the rake support was accounted for by use of the method of reference 2.

RESULTS AND DISCUSSION

The static-pressure-coefficient distribution over the surface of the spinner for various free-stream Mach numbers is shown in figure 3. The rakes caused some interference with the flow near the base of the spinner $\left(\frac{x}{l} = 0.785\right)$. This interference is shown in the plotted data points but is faired out in the curves. The data indicate that the flow over the spinner accelerates from the stagnation point to near free-stream conditions and then decelerates slightly. It was intended that the flow over the spinner accelerate from stagnation to slightly above free-stream velocity and then decelerate through free-stream velocity at the propeller plane. However, blockage caused by the conical fore-body of the fuselage prevented the existence of free-stream conditions in the propeller plane.

The values of static-pressure coefficient shown in figure 3 are the averages of the pressures on the top and bottom surfaces of the spinner at the same value of x/l and, therefore, the effects of the small angles of attack (0° to 1.6°) and the asymmetrical distribution of protuberances around the airplane are disregarded (ref. 1). The maximum $(\text{at } M_\infty = 0.65)$ and minimum $(\text{at } M_\infty = 0.85)$ encountered differences in static pressure due to angle of attack between the top and bottom of the spinner are shown in figures 4(a) and 4(b), respectively.

The variation of local Mach number with radial distance from the spinner surface near the propeller plane at various free-stream Mach numbers is shown in figure 5. The values of M_l/M_∞ shown for the top and bottom rakes indicate the small difference between the two values due to angle of attack. Figure 5 also shows that the desired result of free-stream conditions in the propeller plane was not obtained. The data indicate that, as the free-stream Mach number increased, the deviation of local conditions in the propeller plane from free stream increased. This result is supported by figure 3. Also, figure 5 shows that the influence of the spinner installation and the forebody of the airplane extends a considerable distance from the spinner, so that a large portion of a propeller blade used with this spinner installation would be in a favorable interference region. The upward concavity of the curves is attributed to the influence of the airplane forebody. The increasing concavity with increasing free-stream Mach number indicates that this influence increased with Mach number.

CONCLUDING REMARKS

The surface pressure distribution and the flow field around a dummy, nonrotating, elliptical spinner were investigated in flight over a Mach number range from 0.65 to 0.95.

The results showed that free-stream conditions were approximated from about 15 to 90 percent of the spinner length, but the local Mach number in the propeller plane varied from about 5 percent less than free stream at a Mach number of 0.65 to about 10 percent less than free stream at a Mach number of 0.95.

Langley Research Center,
National Aeronautics and Space Administration,
Langley Field, Va., October 23, 1958.

REFERENCES

1. Hammack, Jerome B., Windler, Milton L., and Scheithauer, Elwood F.: Flight Investigation of the Surface-Pressure Distribution and the Flow Field Around a Conical and Two Spherical Nonrotating Full-Scale Propeller Spinners. NACA TN 3535, 1955.

2. Krause, Lloyd N.: Effects of Pressure-Rake Design Parameters on Static-Pressure Measurement for Rakes Used in Subsonic Free Jets. NACA TN 2520, 1951.

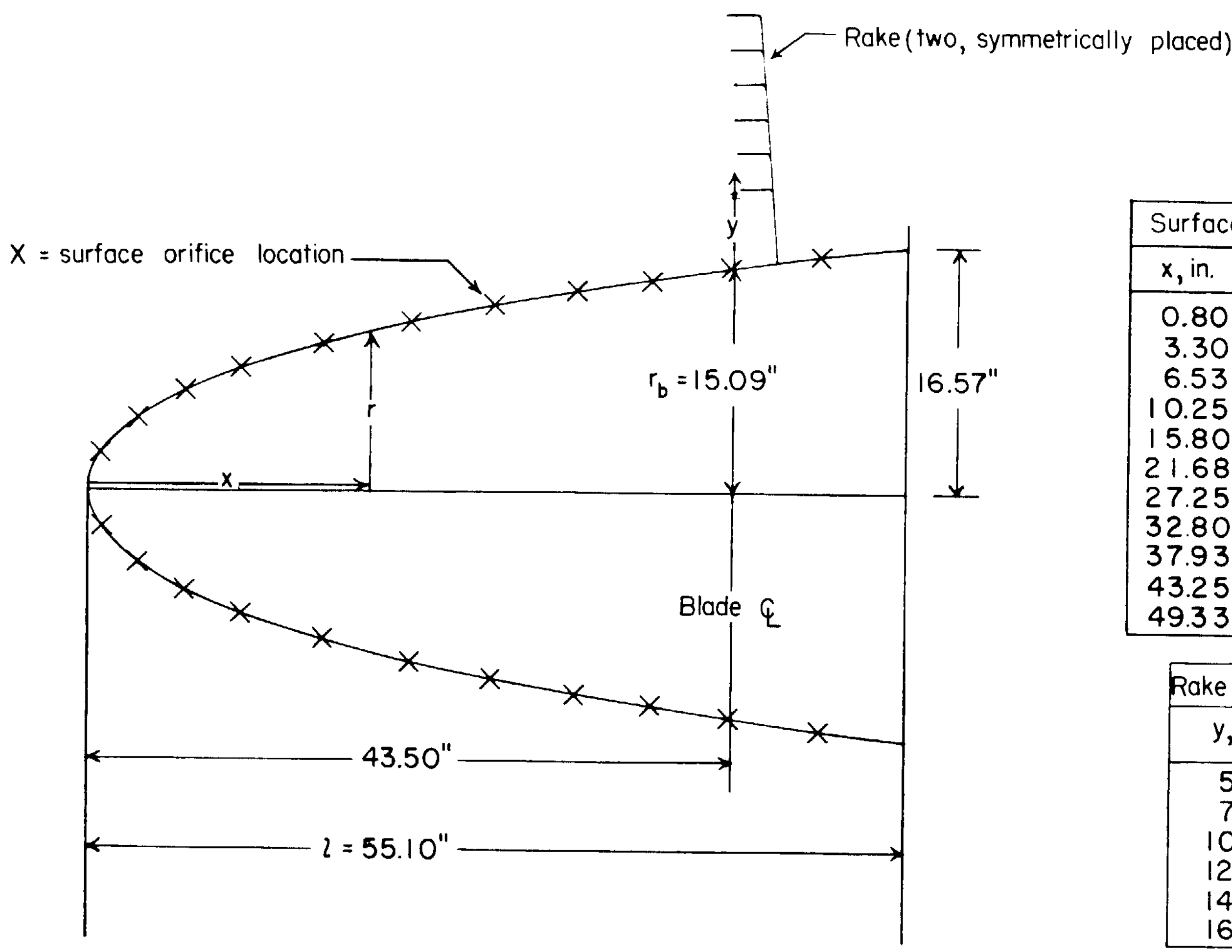

Surface orifice locations		
x, in.	r, in.	x/l
0.80	2.45	0.0145
3.30	4.87	.0599
6.53	6.75	.1185
10.25	8.25	.1860
15.80	9.98	.2868
21.68	11.35	.3935
27.25	12.50	.4946
32.80	13.50	.5953
37.93	14.25	.6884
43.25	15.05	.7849
49.33	15.85	.8953

Rake orifice locations	
y, in.	$\frac{r_b+y}{r_b}$
5.45	1.361
7.79	1.519
10.05	1.666
12.36	1.822
14.74	1.978
16.97	2.125

Figure 1.- Dimensions and orifice locations of the elliptical spinner.

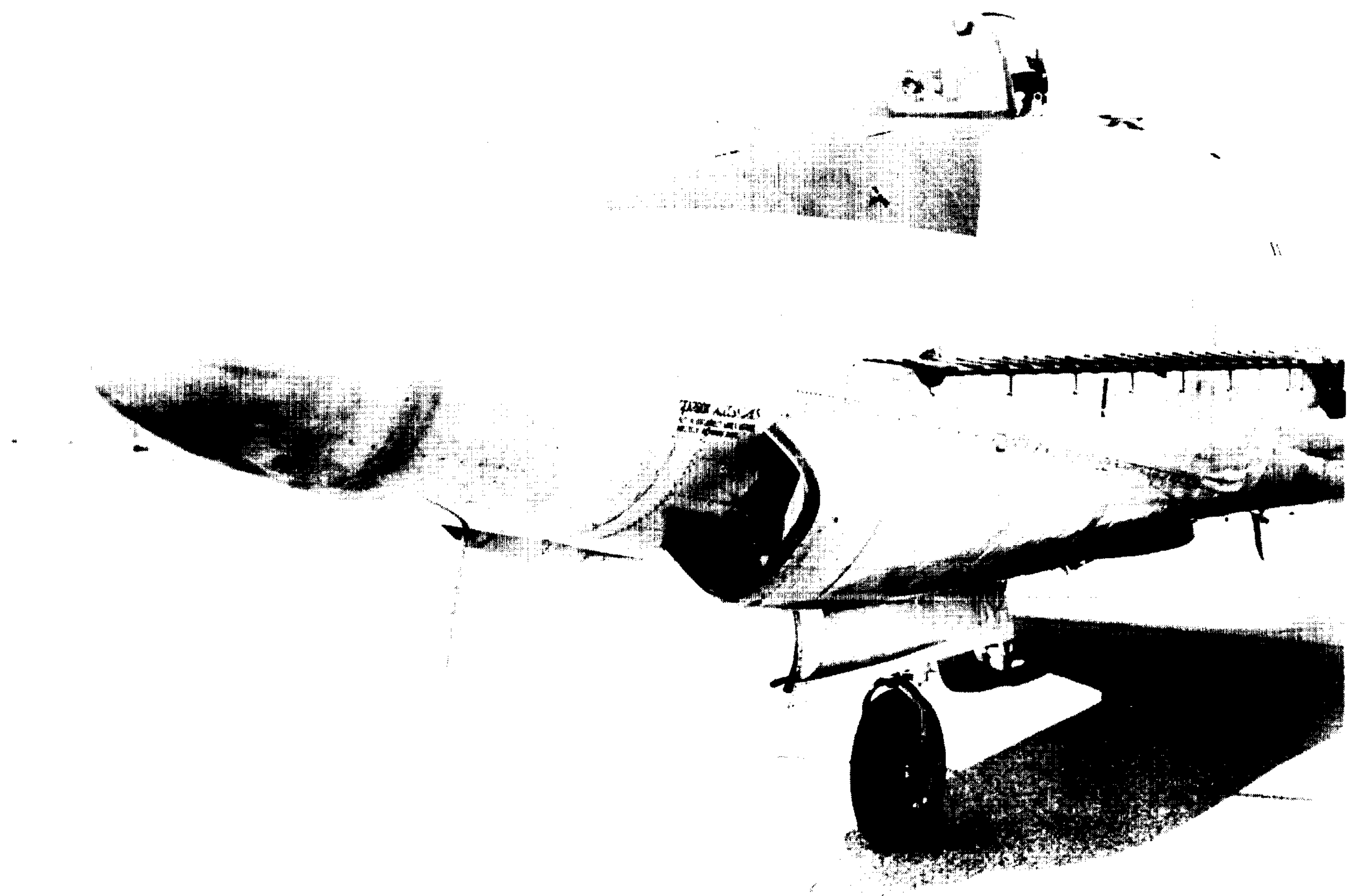

L-57-5167
Figure 2.- Installation of elliptical spinner on propeller research airplane.

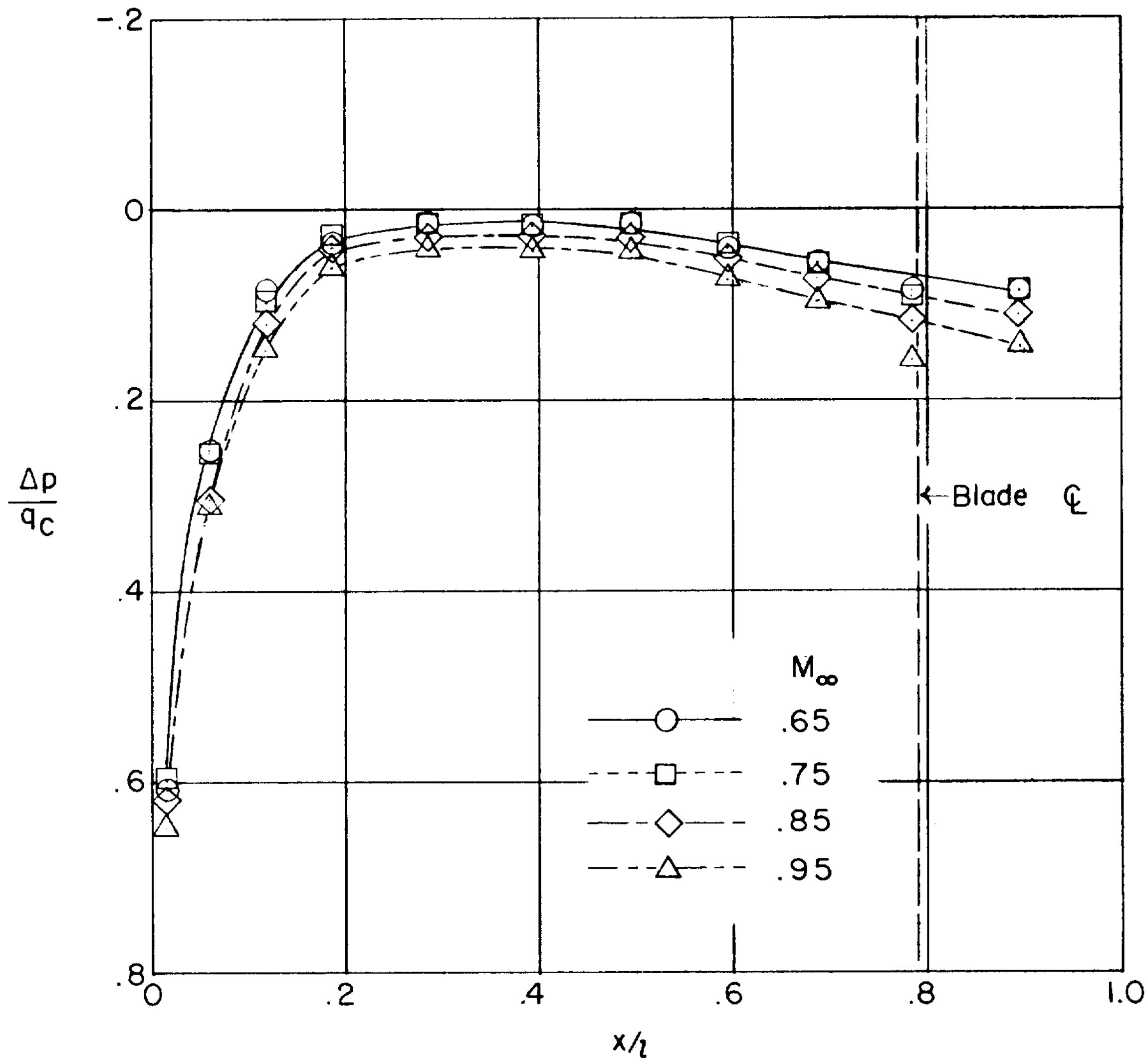

Figure 3.- Static-pressure-coefficient distribution over the surface of the elliptical spinner for various free-stream Mach numbers.

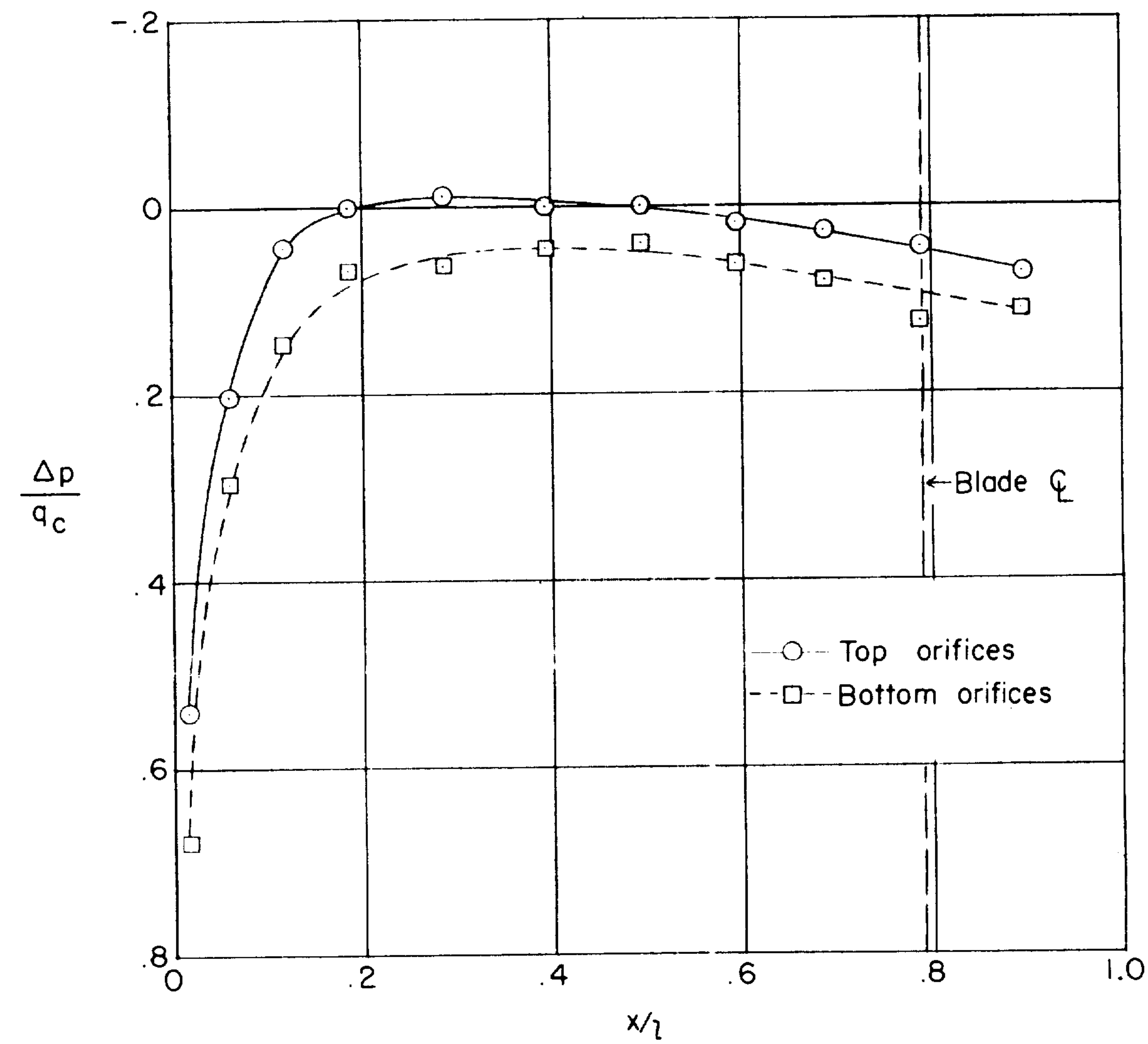

(a) Maximum difference in static-pressure coefficient $\frac{\Delta p}{q_c}$; $M_\infty = 0.65$.

Figure 4.- Examples of differences between static pressures on top and bottom surfaces of the elliptical spinner.

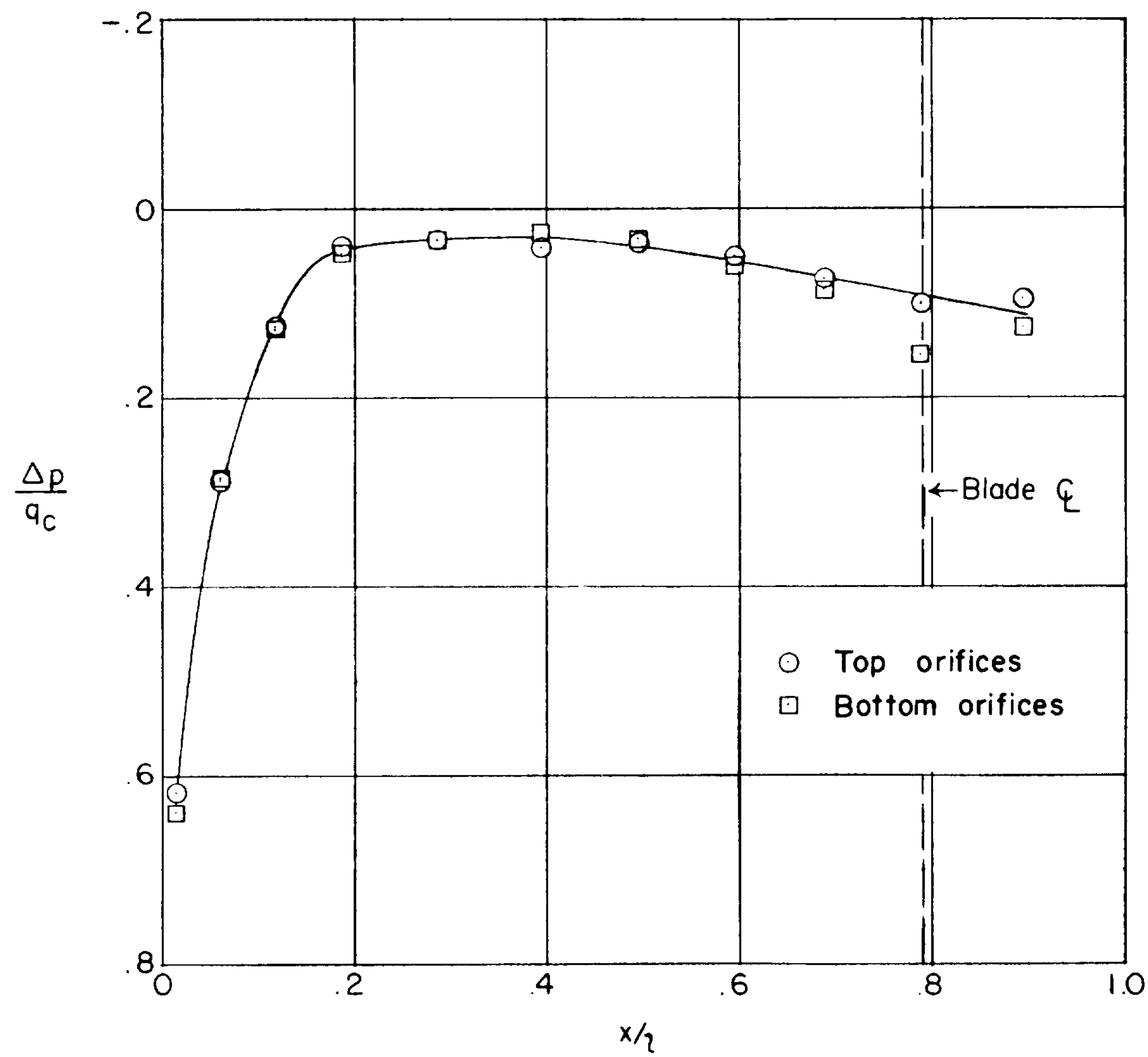

(b) Minimum difference in static-pressure coefficient $\frac{\Delta p}{q_c}$; $M_\infty = 0.85$.

Figure 4.- Concluded.

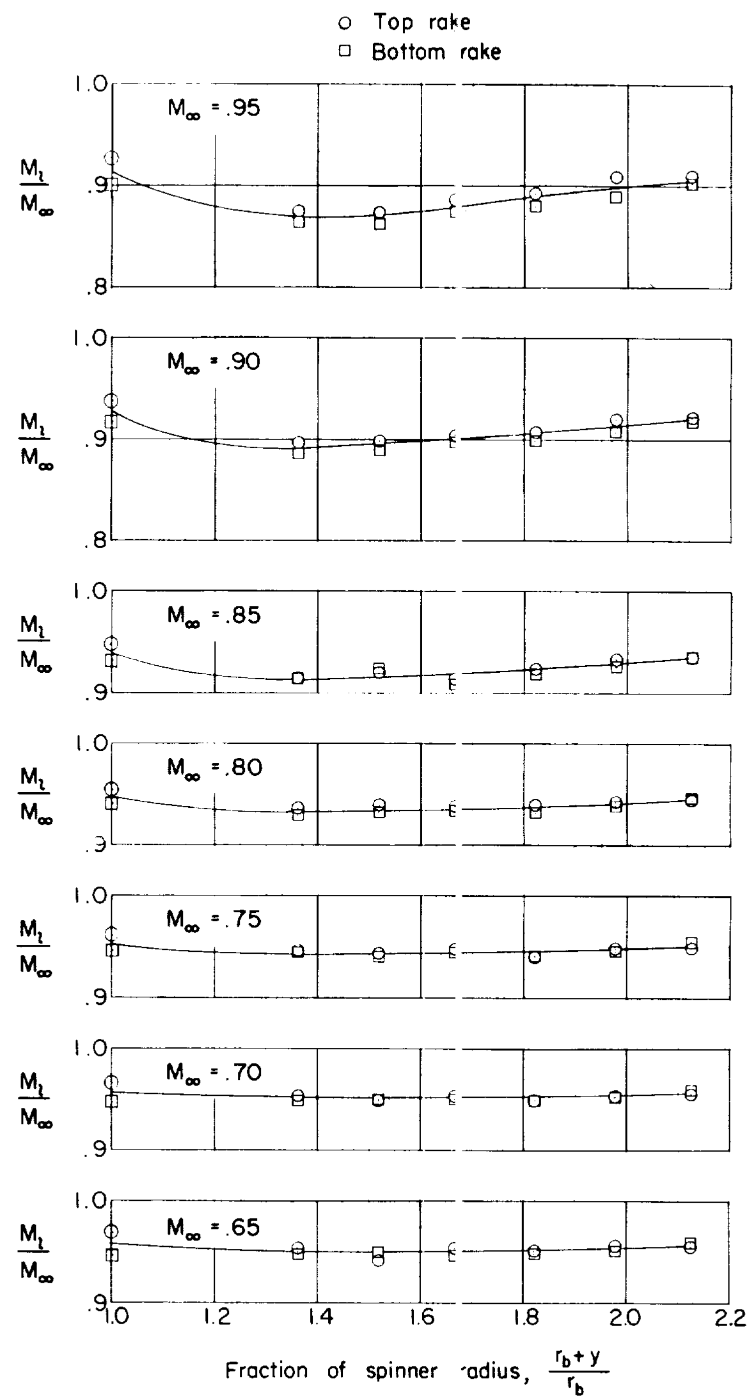

Figure 5.- Variation of local Mach number with radial distance from the spinner surface near the propeller plane at various free-stream Mach numbers.